

131, 1458 (1963).

<sup>45</sup>D. M. T. Newsham, *Phys. Rev.* **152**, 841 (1966).

<sup>46</sup>J. Kuebler and M. P. Tosi, *Phys. Rev.* **137**, A1617 (1965).

<sup>47</sup>E. Somoza and H. Fenichel, *J. Chem. Phys.* **48**, 2382 (1968).

<sup>48</sup>R. H. Gupta and N. P. Gupta, *Nuovo Cimento* **66B**, 1 (1970).

<sup>49</sup>N. S. Gillis, N. R. Werthamer, and T. R. Koehler, *Phys. Rev.* **165**, 951 (1968).

<sup>50</sup>N. R. Werthamer, *Am. J. Phys.* **37**, 763 (1969).

<sup>51</sup>V. V. Goldman, G. K. Horton, and M. L. Klein, *J. Low-Temp. Phys.* **1**, 391 (1969).

<sup>52</sup>J. A. Leake, W. B. Daniels, J. Skalyo, Jr., B. C. Frazer, and G. Shirane, *Phys. Rev.* **181**, 1251 (1969).

PHYSICAL REVIEW B

VOLUME 3, NUMBER 10

15 MAY 1971

## Raman Scattering and Small-Angle X-Ray Scattering in $\text{KCl}_{1-x}\text{Br}_x$ <sup>†</sup>

Indira Nair and Charles T. Walker

*Department of Physics, Northwestern University, Evanston, Illinois 60201*

(Received 2 December 1970)

The Raman spectra of the mixed halide  $\text{KCl}_{1-x}\text{Br}_x$  were studied as a function of concentration. First-order Raman-active phonons of  $A_{1g}$  symmetry were observed at approximately 120 and 145  $\text{cm}^{-1}$  at  $x < 0.3$ . Above this concentration, the 120- $\text{cm}^{-1}$  mode disappeared, leaving the higher-frequency band only in the first-order spectrum. This band was found to shift linearly with concentration and the extrapolation of the straight-line fit intersects the pure-crystal axes at values close to that of the pure-crystal  $\text{TO}(X)$  phonon. At the KBr end of the concentration range, the first-order spectrum resembles the pure-crystal density of states. The first-order spectra of the  $T_{2g}$  symmetry were also studied. These reflect the pure-crystal density of states at both ends of the concentration range. The crystals were also investigated by small-angle x-ray scattering for evidence of clustering. No clusters smaller than  $(30)^3$  unit cells were found. Because of the comparable intensities of the first- and second-order spectra, it was not possible to arrive at perfectly conclusive results.

### I. INTRODUCTION

This paper describes the results of an investigation of the Raman spectra of  $\text{KCl}_{1-x}\text{Br}_x$  for  $1 \geq x \geq 0$ . Mixed crystals of alkali halides have been studied extensively by x-ray and thermodynamic techniques.<sup>1-6</sup> The results of these studies most relevant to the present work are the following: (a)  $\text{KCl-KBr}$  system forms a homogeneous series of continuous solid solutions at all temperatures.<sup>3</sup> (b) The system obeys Vegard's law, i.e., linear dependence of the lattice constants of solid solutions on composition,<sup>4</sup> the agreement being to within 0.08%. The optical phonons of  $\text{KCl}_{1-x}\text{Br}_x$  have been studied by Mitsuishi<sup>7</sup> using thin-film transmission measurements and by Fertel and Perry<sup>8</sup> from a Kramers-Kronig analysis of the reflectivity spectra. Mitsuishi finds a linear variation of the  $\text{TO}$  frequency with composition while the results of Fertel and Perry show a nonlinear variation.

Several theoretical models have been proposed to describe the behavior of phonons in mixed crystals.<sup>9</sup> The first such attempt by Matossi<sup>10</sup> considered a linear diatomic chain model of a 50-50 crystal  $\text{AB}_{1-x}\text{C}_x$  with nearest-neighbor force constants only. This model predicted two modes which are weakly Raman active or inactive depending upon whether the structure of the mixed crystal is peri-

odic or statistical, and one mode which is Raman active in either case. The virtual-crystal model of Langer,<sup>11</sup> in which all masses and force constants are taken as averages weighted by the mixed crystal composition, gives only qualitative results and predicts a linear variation of phonon frequency with composition. These models are one dimensional. However, the qualitative results are similar for one-, two-, and three-dimensional lattices.<sup>12</sup> Verleur and Barker<sup>13</sup> considered a model based on short-range clustering to account for the two-mode behavior of semiconductor mixed crystals. In their model, a one-mode behavior would result when the frequencies of the pure end members are close to each other. The random-element isodisplacement (REI) model of Chen, Shockley, and Pearson<sup>14</sup> considered essentially a unit cell containing one unit of  $\text{AB}_{1-x}\text{C}_x$  and then assumed randomness, i.e., each atom is subjected to forces produced by a statistical average of its neighbors and no effects of order are present. The Grüneisen constant enters the model calculations as a parameter, the force constants  $F_{AB}$  and  $F_{AC}$  at  $x=0$  and  $x=1$  are related to the optic frequencies of the end members  $AB$  and  $AC$ , and a third force constant  $F_{BC}$  is used as an adjustable parameter.

This model has been altered in the modified random-element isodisplacement (MREI) model of

Chang and Mitra.<sup>15</sup> Instead of using the Grüneisen constant or the adjustable parameter  $F_{BC}$ , they subject all force constants to the boundary condition that the model must be valid at  $x=0$  and  $x=1$ , where the optic phonons of the pure compounds and the local or gap mode occur. In the MREI-model calculations for one-mode systems, additional conditions have to be imposed since there are no local or gap modes in these systems. Either the two roots of the secular equation determining the frequencies may be set equal to each other or one root set equal to zero. The second is equivalent to the virtual-crystal approximation, yielding a linear variation of optic frequency with composition, while the first method gives a nonlinear variation.

Mitsubishi's experimental results on KCl:KBr seem to follow the virtual-crystal predictions. However, the composition of the thin films used in the measurements is not accurately known. The results of Fertel and Perry are closely described by the first method except at 80 °K where neither method fits. With the above techniques, however, one can study only the  $k=0$  phonons. The REI models are also long-wavelength limits.

Several mixed-crystal systems have been studied by Raman spectroscopy.<sup>16-21</sup> The experimental observations on Raman scattering from the mixed-fluorite systems by Chang, Lacina, and Pershan<sup>20</sup> represent a beautiful example of type-I behavior, i. e., a single  $k=0$  optic mode which shifts linearly with concentration. In  $\text{Ca}_{1-x}\text{Sr}_x\text{F}_2$ , the high intensity of the first-order Raman line and the large separation ( $\sim 300 \text{ cm}^{-1}$ ) from the Rayleigh-scattered line enabled accurate measurements of frequencies and linewidths. The frequencies measured as a function of the concentration  $x$  were found to lie on the straight line joining the frequencies of the single Raman-active phonons of the end members.

The Raman spectra of KCl-KBr mixed crystals were first studied by Stekhanov and Eliashberg<sup>19</sup> for four values of  $x$ , both at room temperature and at 35 °C. However, neither symmetry assignments nor the clear identification of the features of the spectra as being due to first- and second-order processes were made in their work. Hurrell *et al.*<sup>21</sup> observed Raman scattering from KBr containing 8-mole% KCl. In the present work, we have covered the complete concentration range and have attempted to describe the nature of the Raman-active phonons of the mixed crystals by complementary experiments on Raman scattering and small-angle x-ray scattering.

## II. EXPERIMENTAL

Mixed crystals of  $\text{KCl}_{1-x}\text{Br}_x$  were grown by the Czochralski method. The crystals of KCl:KBr with low doping and near  $x=0.4$  were found to be more easily grown than the ranges  $x=0.1-0.2$  and

$x=0.7-0.9$ . The best crystals were obtained for  $x=0.36$  and  $0.44$ . The composition of the crystals was determined by measuring the macroscopic density using 1, 2- dibromopropane as the flotation liquid. Vegard's law was used to calculate the theoretical density as a function of concentration.

### A. Small-Angle X-Ray Scattering

As will be seen later, the Raman data show a complicated mixture of first- and second-order spectra. In order to be sure that these results were not an artifact of some peculiarities of composition, the crystals were examined for evidence of clustering using small-angle x-ray scattering. Long-range order can be ruled out by the work of Vegard,<sup>5</sup> Tobolsky,<sup>3</sup> and others.<sup>1</sup> Both photographic and scintillation counter detection were utilized. The intensity of small-angle scattering owing to clustering in the KCl-KBr system may be expected to be very weak. To calculate the magnitudes involved, the approximate formula (Ref. 22, p. 326) for the scattering power per cluster as a function of the angle of scattering

$$I(s) = (\rho - \rho_0)^2 R^6 e^{-4\pi^2 s^2 R^2}$$

(where  $s = 2\theta/\lambda$ ) was used. This assumes a model of cubic clusters of side  $R$  of the material with average electron density  $\rho$  embedded in a medium of electron density  $\rho_0$ . This calculation neglects absorption and the variation of lattice parameter with composition. To obtain the experimentally observed intensity, the above equation has to be multiplied by  $E$ , where

$$E = I_0 V (N/d^2) \eta;$$

$I_0$  is the incident intensity,  $V$  is the effective volume of the sample,  $d$  is the distance from sample to detector,  $N$  is the number of clusters per unit volume, and  $\eta$  is the detection efficiency.

This indicates that the angular half-width of the scattered beam depends only on  $R$ , i. e., on the cluster size, being larger for small clusters. The peak intensity ( $2\theta=0$ ) is, however, dependent on the number of clusters per unit volume, which in turn depends on the percentage composition. For clusters of the size of 8 unit cells of KBr and KCl, the full width at half-maximum of the scattered peak is  $2 \times 0.88^\circ$ . The peak intensity for the same cluster size is approximately 5000 counts/sec for  $x=0.5$  and 2000 counts/sec for  $x=0.2$  for a source-to-sample distance of 200 mm. The slit widths and distances were chosen so as to obtain maximum intensity with reasonable resolution. Both slow scans and point counting were done with the counter, and long-exposure photographs were taken with an evacuated camera. For the photographs, beam interceptors of optimum width calculated from the

corresponding geometry were used.

Since the scattering was to be observed in transmission, absorption had to be minimized, and hence very thin samples of the mixed crystals ( $\sim 0.003$  cm thick) were required. Samples were cleaved down to a thickness of about 1 mm, etched down to required size with a water and alcohol solution, and washed in alcohol. The samples were then annealed in an argon atmosphere at  $620^\circ\text{C}$  for 12 h. This treatment is required to remove the composition differences brought about by the difference in solubility in alcohol and water of KCl and KBr.<sup>23</sup> It was observed that water etching without annealing gave rise to a spurious peak, as reported by Luova.<sup>24</sup> The edges of the thinned samples were glued between two aluminum foils with suitable slits cut in them and the foil then mounted in the sample holder in the goniometer.

#### B. Raman Scattering

The Raman spectra were taken using a Spex Double Monochromator with photon-counting detector, and a coherent radiation model 52 argon laser. The usual  $90^\circ$  geometry was used and polarizations of the incident and scattered light were selected as described by Krauzman<sup>25</sup> to enable separate observation of the phonon symmetries ( $A_{1g} + 4E_g$ ),  $T_{2g}$  alone, or  $E_g$  alone.

### III. RESULTS AND DISCUSSION

The density measurements indicated that the crystals contained a greater ratio of Cl:Br than the starting material, as was to be expected because of the different melting points of the salts. It is known that the microscopic density varies as much as 7% from the macrodensity.<sup>1,4</sup> This implies that there could be local variations of as much as 20% in the composition, a conclusion that has also been drawn from color-center studies.<sup>26</sup>

#### A. Small-Angle X-Ray Scattering

Samples with  $x = 0.16$ ,  $0.36$ , and  $0.44$  were examined for clustering. Since both slow scanning and point counting with a scintillation counter failed to reveal any small-angle scattering, long-exposure

photographs with an evacuated camera, using a minimum sample-film distance, were taken. To illustrate the results obtained, the photographs for a particular geometry chosen to detect clusters smaller than  $(10)^3$  unit cells are shown in Fig. 1. The angular half-width used for the interceptor corresponded to  $0.3^\circ$ . Figures 1(a) and 1(b) are photographs taken with no sample and with a sample of  $\text{KCl}_{0.2}\text{Br}_{0.8}$ , respectively. Figure 1(c) shows the small-angle scattering from the alloy Al-23% Zn and has been included to demonstrate a typical small-angle scattering peak. No small-angle scattering is observed from our mixed crystal. Similar photographs were taken for settings designed for better resolution. No evidence of clusters smaller than  $(30)^3$  unit cells was found.

The Bragg peaks for the samples were broad, indicating an imperfect crystal. Obviously, the broadening results from both the misalignment of crystal planes and other imperfections as well as composition differences. Assuming all of it arose from composition difference, the maximum peak width corresponded to a composition variation of 20%. As indicated above, past studies<sup>3,24</sup> have shown that there is no long-range order in the KCl-KBr system, and clustering is ruled out by the present experiment.

#### B. Raman Scattering

The room-temperature Raman spectra of pure KCl and KBr and those of the mixed crystals as a function of composition are shown in Fig. 2. These spectra were taken with the crystal oriented so as to observe the  $(A_{1g} + 4E_g)$  spectra. The  $E_g$  spectrum alone is only about 5% as intense as the  $A_{1g} + 4E_g$  spectrum, and is localized around  $120\text{ cm}^{-1}$ . Hence these spectra may be taken to be completely due to individual phonons and phonon combinations of  $A_{1g}$  symmetry.

The second-order spectrum of pure KCl has been reported previously by Krauzman,<sup>27</sup> and our results are in agreement with his. The strongest peak, as seen in Fig. 2, for pure KCl is the band at  $298\text{ cm}^{-1}$ , corresponding presumably to the superposition of the combination bands  $2\text{TO}$ ,  $\text{LO} + \text{TO}$ , and  $2\text{LO}$ .

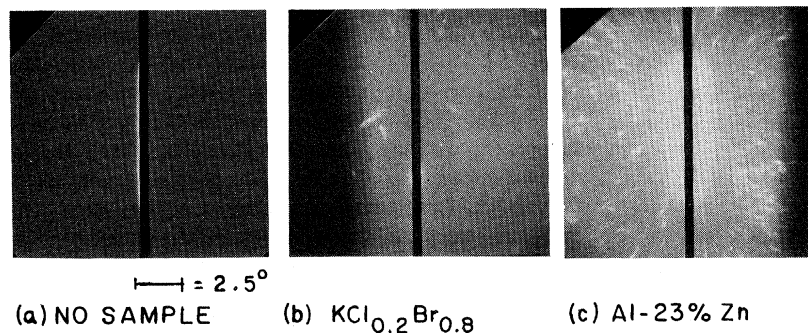


FIG. 1. Photographs of small-angle x-ray scattering patterns with interceptor corresponding to  $2\theta = 0.25^\circ$ . (a) No sample. Slight shadow indicates small misalignment of interceptor. (b) Sample:  $\text{KCl}_{0.2}\text{Br}_{0.8}$ . No evidence of small-angle scattering. (c) Sample: Al-23% Zn alloy showing clearly the small-angle scattering pattern.

(as deduced from the neutron data<sup>28</sup> for KCl). No change in this peak or indeed in the KCl spectrum generally is evident for  $x=0.001, 0.01$ . The first noticeable change occurs at  $x=0.05$  (5% KBr in KCl). A band at  $120 \pm 3 \text{ cm}^{-1}$  appears as the strongest feature of the spectrum; it is a superposition of a KCl second-order peak plus a peak from the mixed crystal. The peak near  $298 \text{ cm}^{-1}$  shifts to  $\sim 292 \text{ cm}^{-1}$ . At liquid-nitrogen temperatures, the  $120\text{-cm}^{-1}$  band can be resolved into a first-order peak (determined from the temperature dependence) and a second-order band. The first-order peak can only be a mode in the mixed crystal while the second-order band is probably a  $2TA(X)$  combination. The  $120\text{-cm}^{-1}$  band continues to be the strongest feature of the spectrum until  $x=0.2$ , by which time it has shifted from  $120$  to  $\sim 115 \text{ cm}^{-1}$ .

At  $x=0.16$ , another peak appears at  $148 \text{ cm}^{-1}$ , which shifts to lower energies and grows in intensity as the proportion of KBr is increased. At  $x=0.3$ , the  $120\text{-cm}^{-1}$  peak is noticeably less intense than this new second peak, now at  $143 \text{ cm}^{-1}$ . A broad feature also now appears distinctly at  $\sim 75 \text{ cm}^{-1}$ . A study of the temperature dependence (Fig. 3) indicates that the  $148\text{-}$  and  $115\text{-cm}^{-1}$  peaks are due to

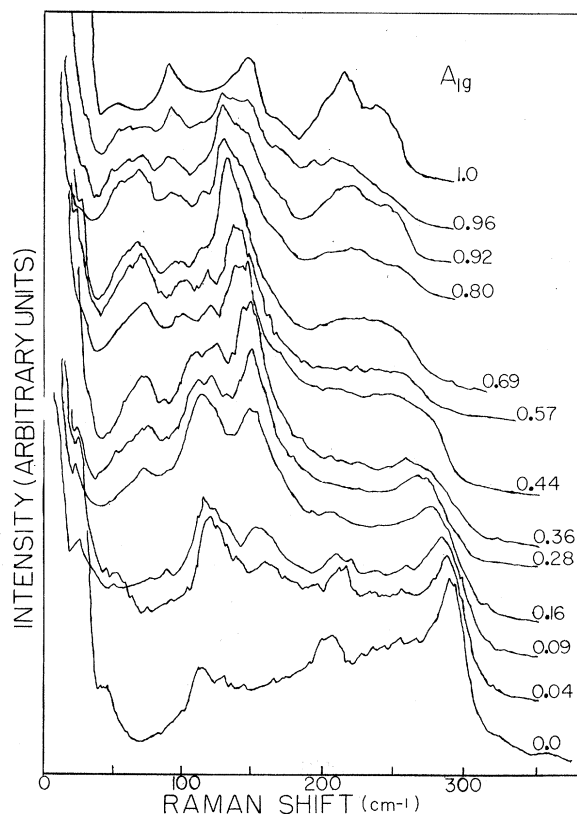


FIG. 2. Room-temperature Raman spectra of  $A_{1g}$  symmetry. The numbers indicate the values of  $x$  for the corresponding samples. Spectral resolution equal to  $3 \text{ cm}^{-1}$ .

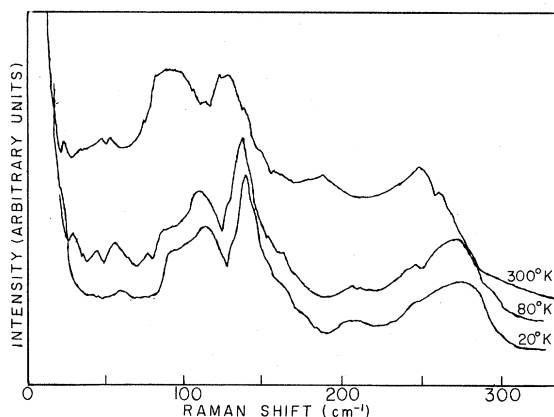


FIG. 3. Raman spectra ( $A_{1g}$ ) of  $\text{KCl}_{0.84}\text{Br}_{0.16}$  at 300, 80, and  $20^\circ\text{K}$ .

first-order processes while the  $75\text{-cm}^{-1}$  band is a second-order band. The resolution of the bands is complicated by the fact that the first- and second-order spectra are comparable in intensity at room temperature and their superposition gives rise to very broad features. Hence the determination of the systematics of linewidths or line shapes is impossible.

Raman spectra of samples cut from different regions of the boule were identical in peak positions and features, indicating an average homogeneity in spite of the expected local variations in composition. Reannealing the samples and taking Raman spectra, or sudden cooling after maintaining them at  $50^\circ\text{K}$  below the melting point for 12 h and then taking the Raman spectra, gave identical results. In frequency values, our results are compatible with those of Stekhanov, and the spectrum for  $x=0.9$  compares well with that of Hurrell *et al.*<sup>21</sup>

The cutoff frequency of the second-order background decreases in intensity with increasing  $x$ . This clearly indicates that the observed spectrum is due to mixed-crystal phonons and their combinations rather than a superposition of KCl and KBr spectra. The most striking effect one would expect at a low concentration of Br (Cl) in KCl (Br) is appearance of first-order Raman lines induced by a breakdown of translational symmetry of the crystal and hence of the  $k=0$  selection rule for Raman scattering. If the substituting halogen ion were truly an isotopic impurity, then the low-concentration crystals should yield a first-order spectrum reflecting the density of states of the pure crystal, as was strikingly demonstrated in Tl-doped potassium halides by Harley *et al.*<sup>29</sup> at a concentration of Tl  $\sim 0.1$  mole%. In the present work, no change in the KCl spectrum was observed at  $x < 0.05$ . On the other hand, the observed first-order phonons for values of  $x$  between 0.1 and 0.8 are phonons of the mixed crystal, the random mixing destroying the

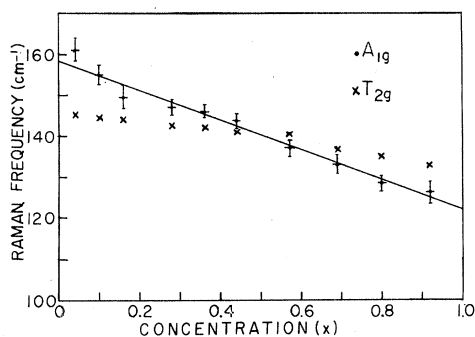


FIG. 4. Dependence of first-order Raman frequencies on composition.

translational symmetry and allowing first-order Raman activity. As  $x$  approaches 1, particularly in the case  $x = 0.8$  and  $0.92$ , the first-order spectrum corresponds closely to the predominant peak of the  $A_{1g}$  density of states of pure KBr.

The low-frequency mode ( $\sim 120 \text{ cm}^{-1}$ ) observed in  $\text{KCl}_{1-x}\text{Br}_x$  for  $x < 0.3$  appears very broad ( $\sim 40 \text{ cm}^{-1}$ ) even though definite bandwidth measurement is not possible. This is probably a resonant mode of  $\text{Br}^-$  in KCl. Weber and Siebert<sup>30</sup> in a far-infrared study have observed a region of large absorption near  $100\text{--}110 \text{ cm}^{-1}$ . Since this band was observed both in  $\text{KCl}:\text{Br}^-$  (0.1 mole%) and  $\text{KCl}:\text{Cu}^+$ , and no temperature dependence was found between 4 and  $52^\circ\text{K}$ , they concluded that it is due to a peak in the density of states of the pure crystal. Karlsson<sup>31</sup> observed a contribution to the specific heat of  $\text{KCl}:\text{Br}$  which he attributed to a resonant mode at  $110 \pm 10 \text{ cm}^{-1}$ . However, impurity specific-heat contributions cannot come from modes of even parity, while the band observed in the present work is definitely of  $A_{1g}$  symmetry.

The pure-crystal density of states, as calculated by Page,<sup>32</sup> shows a density-of-states peak for  $A_{1g}$  symmetry at  $\sim 118 \text{ cm}^{-1}$ ; however, there is a much stronger peak at  $148 \text{ cm}^{-1}$ . In view of this, it would seem that the  $120\text{-cm}^{-1}$  Raman peak is the result of scattering by a resonant mode of  $\text{Br}^-$  in KCl rather than being merely a reflection of the density of states. Its decreasing intensity as concentration of KBr increases above 20% is also suggestive of its being a resonant mode, since at such high concentrations the mode should broaden into an impurity band.

The variation of the second first-order line (near  $148 \text{ cm}^{-1}$ ) in  $\text{KCl}_{1-x}\text{Br}_x$  with composition is shown in Fig. 4. The variation is approximately linear. If it is assumed to be linear, the straight-line fit would cut the  $x = 0$  (KCl) and  $x = 1$  (KBr) axes at  $155 \pm 3$  and  $125 \pm 3 \text{ cm}^{-1}$ , respectively. A long-wavelength theory, such as the MREI model of Chang and Mitra, would give a nonlinear variation. Its applicability here, however, is doubtful since the

$k = 0$  selection rule need not hold in the mixed crystals. It is tempting to note that the intersection values at the pure crystals correspond closely to the TO frequencies of KCl and KBr at the  $X$  point,<sup>28,33</sup> which are  $156$  and  $120 \text{ cm}^{-1}$ , respectively. However, the neutron data for KCl were taken at  $118^\circ\text{K}$ , and cannot be directly compared with our Raman data taken at room temperature. The neutron data corrected to room temperature should probably be closer to  $152$  and  $120 \text{ cm}^{-1}$ , respectively. Thus the first-order line observed could be the  $\text{TO}(X)$  phonon of the mixed crystals but this identification is not unambiguous. For example, near the extreme values of  $x$ , this spectral region is probably also enhanced by the fact that the strongest peaks in  $A_{1g}$  density of states in pure KCl and KBr are at  $150$  and  $130 \text{ cm}^{-1}$ , respectively. In fact, as  $x$  approaches 1, in particular in the case of  $x = 0.8$  and  $0.92$ , the first-order peak of the spectrum corresponds closely to the predominant peak of the  $A_{1g}$  density of states for pure KBr, as calculated by Page. Therefore, it is not possible to identify this peak unambiguously as being either the TO phonon at  $X$ , or a peak in the density of states from other phonon critical points.

The  $T_{2g}$  phonons were also studied as a function of concentration. The  $T_{2g}$  Raman spectra are shown in Fig. 5 and the frequency variation of the

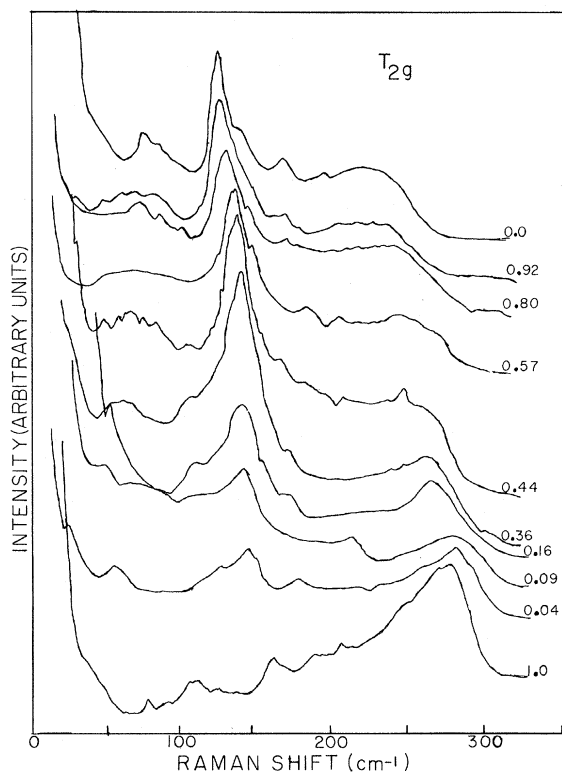


FIG. 5. Room-temperature Raman spectra of  $T_{2g}$  symmetry.

first-order line in Fig. 4. At low-Br concentrations, the first-order spectrum is a band centered at  $145\text{ cm}^{-1}$ , resembling the peak in the density of states of  $T_{2g}$  phonons in pure KCl. This band shifts very little in frequency as concentration is varied up to  $x=0.5$  and then falls gradually down to  $133\text{ cm}^{-1}$  for  $x=0.92$ . The density of states for pure KBr has a high region  $105\text{--}140\text{ cm}^{-1}$  with peaks at  $121$  and  $130\text{ cm}^{-1}$ . The resolution of the nature of the peaks in this region is complicated by the fact that the  $T_{2g}$  Raman spectrum of pure KBr consists predominantly of a band in the region  $115\text{--}135\text{ cm}^{-1}$  arising mainly from the combination LA+TA( $\Delta$ ). Thus the first-order Raman spectrum near  $x=1$ , the density of states curve for pure KBr, and the second-order Raman spectrum of pure KBr fall in the same region, making any comments on the  $T_{2g}$  spectra risky at best.

#### IV. CONCLUSIONS

It is interesting to note that zone-edge phonons seem to be predominant in first-order Raman scat-

tering from the mixed crystals. Conclusive results cannot be drawn from the Raman data for  $\text{KCl}_{1-x}\text{Br}_x$  because of the comparable intensity of first- and second-order Raman scattering. An average Green's-function approach similar to that of Pershal and Lacina<sup>34</sup> may be instructive in deciding whether the first-order spectrum observed is a reflection of the mixed-crystal density of states. Other alkali-halide systems which form solid solutions over fairly large regions of concentration are being presently studied by Raman and x-ray scattering techniques in the hope that one might be able to follow the behavior of the phonons as they evolve from those of one pure end member to the other.

#### ACKNOWLEDGMENTS

We should like to thank Professor J. B. Cohen of the Material Science Department for guidance in the x-ray work and for the use of his equipment, Dr. J. B. Page, Jr., for the density-of-states curves, and R. Gonzales for growing the mixed crystals.

<sup>†</sup>Work supported by the Army Research Office, Durham, N. C. and by the Advanced Research Projects Agency through the Northwestern University Materials Research Center.

<sup>1</sup>P. Luova, Ann. Acad. Sci. Fennicae **A155** (1964).

<sup>2</sup>F. A. Matsen and J. Y. Beach, J. Am. Chem. Soc. **63**, 3470 (1941).

<sup>3</sup>A. V. Tobolsky, J. Chem. Phys. **10**, 187 (1942).

<sup>4</sup>A. Smakula, N. Maynard, and A. Repucci, J. Appl. Phys. **S33**, 453 (1962).

<sup>5</sup>L. Vegard, Z. Physik **5**, 17 (1921).

<sup>6</sup>M. Ahtee, Ann. Acad. Sci. Fennicae **AV1** (No. 313) (1969).

<sup>7</sup>A. Mitsuishi, in U. S. Japan Cooperative Seminar on Far Infrared Spectroscopy, Columbus, Ohio, 1965 (unpublished).

<sup>8</sup>J. H. Fertel and C. H. Perry, Phys. Rev. **184**, 874 (1969).

<sup>9</sup>G. Lucovsky, M. Brodsky, and E. Burstein, in *Localized Excitations in Solids*, edited by R. F. Wallis (Plenum, New York, 1968), p. 592.

<sup>10</sup>F. Matossi, J. Chem. Phys. **19**, 161 (1951).

<sup>11</sup>J. S. Langer, J. Math. Phys. **2**, 584 (1961).

<sup>12</sup>P. Dean, in *Lattice Dynamics*, edited by R. F. Wallis (Pergamon, New York, 1965), p. 561.

<sup>13</sup>H. W. Verleur and A. S. Barker, Phys. Rev. **149**, 715 (1966).

<sup>14</sup>Y. S. Chen, W. Shockley, and G. L. Pearson, Phys. Rev. **151**, 648 (1966).

<sup>15</sup>I. F. Chang and S. S. Mitra, Phys. Rev. **172**, 924 (1968).

<sup>16</sup>O. Brafman, I. F. Chang, G. Lengyel, S. S. Mitra,

and E. Carnall, Phys. Rev. Letters **19**, 1120 (1967).

<sup>17</sup>G. H. Perry and N. E. Tornberg, Phys. Rev. **183**, 595 (1969).

<sup>18</sup>D. W. Feldman, M. Ashkin, and J. H. Parker, Jr., Phys. Rev. Letters **17**, 1209 (1966).

<sup>19</sup>A. I. Stekhanov and M. B. Eliashberg, Opt. i Spektroskopiya **X**, 348 (1961) [Opt. Spectry. (USSR) **10**, 174 (1961)].

<sup>20</sup>R. K. Chang, B. Lacina, and P. S. Pershan, Phys. Rev. Letters **17**, 755 (1966).

<sup>21</sup>J. P. Hurrell, S. P. S. Porto, T. C. Damen, and S. Mascarenhas, Phys. Letters **26A**, 194 (1968).

<sup>22</sup>A. Guinier, *X-Ray Diffraction* (Freeman, San Francisco, 1963).

<sup>23</sup>M. Sakamoto and S. Kobayashi, J. Phys. Soc. Japan **13**, 1231 (1958).

<sup>24</sup>P. Luova, Suomen Kemistilehti **B36**, 139 (1963).

<sup>25</sup>M. Krauzman, Compt. Rend. **265B**, 689 (1967).

<sup>26</sup>G. Meissner, Z. Physik **134**, 604 (1953).

<sup>27</sup>M. Krauzman, in *Light-Scattering Spectra of Solids*, edited by G. B. Wright (Springer-Verlag, Berlin, 1969).

<sup>28</sup>J. R. D. Copley, R. W. Macpherson, and T. Timusk, Phys. Rev. **182**, 965 (1969).

<sup>29</sup>R. T. Harley, J. B. Page, Jr., and C. T. Walker, Phys. Rev. Letters **23**, 922 (1969).

<sup>30</sup>R. Weber and F. Siebert, Z. Physik **213**, 273 (1968).

<sup>31</sup>A. V. Karlsson, Phys. Rev. B (to be published).

<sup>32</sup>J. B. Page, Jr. (private communication).

<sup>33</sup>A. D. B. Woods, B. N. Brockhouse, R. A. Cowley, and W. Cochran, Phys. Rev. **131**, 1025 (1963).

<sup>34</sup>P. S. Pershan and W. B. Lacina, Phys. Rev. **168**, 725 (1968).

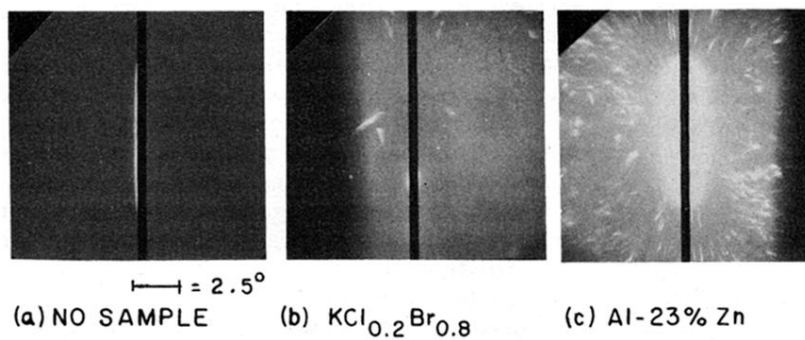


FIG. 1. Photographs of small-angle x-ray scattering patterns with intercept corresponding to  $2\theta = 0.25^\circ$ . (a) No sample. Slight shadow indicates small misalignment of intercept. (b) Sample:  $\text{KCl}_{0.2}\text{Br}_{0.8}$ . No evidence of small-angle scattering. (c) Sample: Al-23% Zn alloy showing clearly the small-angle scattering pattern.